

TaO⁺, a Candidate Molecular Ion in Search of Physics Beyond the Standard Model

Timo Fleig^{1,*}

¹*Laboratoire de Chimie et Physique Quantiques,
I.R.S.A.M.C., Université Paul Sabatier Toulouse III,
118 Route de Narbonne, F-31062 Toulouse, France*

(Dated: February 26, 2018)

The TaO⁺ molecular ion is proposed as a candidate system for detecting signatures of charge parity (\mathcal{CP}) violating physics beyond the standard model of elementary particles. The electron electric dipole moment (EDM) effective electric field $E_{\text{eff}} = 20.2 \left[\frac{\text{GV}}{\text{cm}} \right]$, the nucleon-electron scalar-pseudoscalar (ne-SPS) interaction constant $W_S = 17.7 \text{ [kHz]}$ and the nuclear magnetic quadrupole interaction constant $W_M = 0.45 \left[\frac{10^{33} \text{ Hz}}{e \text{ cm}^2} \right]$ are found to be sizeable \mathcal{P} , \mathcal{T} -odd enhancements. The ratio of the leptonic and semi-leptonic enhancements differs strongly from the one for the ThO system which may provide improved limits on the electron EDM, d_e , and the SPS coupling constant, C_S . TaO⁺ is found to have a $^3\Delta_1$ electronic ground state like the previously proposed ThF⁺ molecular ion, but an order of magnitude smaller parallel G-tensor component which makes it less vulnerable to systematic errors in experiment.

INTRODUCTION

In the search for physics beyond the standard model (BSM) of elementary particles electric dipole moments (EDMs) of atomic and molecular systems are a powerful probe in the low-energy regime [1]. The corresponding spatial parity (\mathcal{P}) and time-reversal (\mathcal{T}) non-conserving interactions may have multiple fundamental sources [2–4] and are themselves, assuming $\mathcal{CP}\mathcal{T}$ -conservation, manifestations of charge-parity (\mathcal{CP}) violation beyond that already incorporated into the SM [5].

Due to the possibility of having different sources contribute to a \mathcal{P}, \mathcal{T} -odd effect in an atomic-scale system, ideally multiple positive measurements on different systems with different dependency on underlying sources should be sought for [6, 7]. One way of making progress is, therefore, the investigation of new systems that display favorable physical properties in the search for EDMs.

Measurements and many-body calculations on electronically paramagnetic molecular systems with low-lying ${}^3\Delta_1$ electronic states currently lead to strong constraints on the electron electric dipole moment, d_e , and the scalar-pseudoscalar nucleon-electron coupling constant, C_S [8–11]. In addition, this kind of paramagnetic molecules also allows for constraining \mathcal{P}, \mathcal{T} -odd hadron physics, originating in the quantum chromodynamics (QCD) (\mathcal{CP})-violating parameter $\tilde{\Theta}$ [12], EDMs of the u and d quarks, $d_{u,d}$, and *via* chromo-EDMs, $\tilde{d}_{u,d}$ [13]. In this context, the interaction of a nuclear magnetic quadrupole moment (MQM) with electronic magnetic fields has been addressed for molecules containing strongly deformed thorium and tantalum nuclei [14–17].

In the present paper, the TaO^+ molecular ion is investigated with four-component relativistic all-electron methods including the effects of inter-electron correlations and proposed as a promising candidate system for measurement of an EDM or for further constraining (\mathcal{CP})-odd BSM parameters through an experimental null result. Molecular properties for low-lying electronic states as well as relevant \mathcal{P}, \mathcal{T} -odd interaction constants for the potential “science state”, ${}^3\Delta_1$, are presented.

METHODS

The electron EDM interaction constant is evaluated as proposed in stratagem II of Lindroth et al. [18] as an effective one-electron operator via the squared electronic momentum operator,

$$E_{\text{eff}} := \frac{2\iota c}{e\hbar} \langle \Psi_\Omega | \sum_{j=1}^n \gamma_j^0 \gamma_j^5 \vec{p}_j^2 | \Psi_\Omega \rangle \quad (1)$$

with n the number of electrons and j an electron index, as described in greater detail in reference [19]. The EDM effective electric field is related to the electron EDM interaction constant $W_d = -\frac{1}{\Omega} E_{\text{eff}}$.

The ne-SPS interaction constant is defined and implemented [20] as

$$W_S := \frac{\iota}{\Omega} \frac{G_F}{\sqrt{2}} Z \langle \Psi_\Omega | \sum_{j=1}^n \gamma_j^0 \gamma_j^5 \rho_K(\vec{r}_j) | \Psi_\Omega \rangle \quad (2)$$

where G_F is the Fermi constant, Z is the proton number and $\rho_K(\vec{r}_j)$ is the nuclear charge density at position \vec{r}_j , normalized to unity.

The parallel magnetic hyperfine interaction constant is defined as follows:

$$A_{||} = \frac{\mu_K}{I\Omega} \langle \Psi_\Omega | \sum_{i=1}^n \left(\frac{\vec{\alpha}_i \times \vec{r}_{iK}}{r_{iK}^3} \right)_z | \Psi_\Omega \rangle \quad (3)$$

where $\vec{\alpha}$ is a vector of Dirac matrices and \vec{r}_{iK} is the position vector relative to nucleus K . Further details can be found in reference [11].

The nuclear MQM interaction constant has been implemented in reference [14] and can be written as

$$W_M = \frac{3}{2\Omega} \langle \Psi_\Omega | -\frac{1}{3} \sum_{j=1}^n \left\{ \left[\alpha_1(j) \frac{\partial}{\partial r_2(j)} - \alpha_2(j) \frac{\partial}{\partial r_1(j)} \right] \frac{r_3(j)}{r^3(j)} \right\} | \Psi_\Omega \rangle. \quad (4)$$

In this case, $r_k(j)$ denotes the k -th cartesian component of vector \mathbf{r} for particle j (*idem* for α).

Finally, the parallel component of the electronic G-tensor for a linear molecule is defined as

$$G_{||} = \frac{1}{\Omega} \left\langle \Psi_{\Omega} | \hat{L}_{\hat{n}}^e + g_s \hat{S}_{\hat{n}}^e | \Psi_{\Omega} \right\rangle \quad (5)$$

for the N -electron wavefunction Ψ_{Ω} in irreducible representation Ω , with $\hat{L}_{\hat{n}}^e = \hat{\mathbf{L}}^e \cdot \hat{n}$ where \hat{n} is a unit vector along the molecular axis and $g_s = -g_e = 2.00231930436182$ is the free-electron g-factor [21].

RESULTS

Technical details

A local version of the DIRAC15 program packages [22, 23] has been used for all presented calculations, extended to allow for the calculation of expectation values over the various reported property operators [11, 14, 19, 20]. In all calculations the speed of light was set to 137.0359998 a.u.

Fully uncontracted all-electron atomic Gaussian basis sets of triple- ζ quality were used for the description of electronic shells, in the case of tantalum Dyll's basis set [24, 25] and for oxygen the Dunning cc-pVTZ-DK set [26]. For tantalum valence- and core-correlating exponents were added, amounting to $\{30s, 24p, 15d, 11f, 3g, 1h\}$ uncontracted functions. In electron-correlated calculations the virtual spinor space has been truncated at 30 a.u.

The two correlated wavefunction models used in the present work, for which the Dirac-Coulomb Hamiltonian

$$\hat{H}^{DC} = \sum_A \sum_i^N [c(\vec{\alpha} \cdot \vec{p})_i + \beta_i m_0 c^2 + V_{iA} \mathbb{1}_4] + \sum_{i,j>i}^N \frac{1}{r_{ij}} \mathbb{1}_4 + \sum_{A,B>A} V_{AB}, \quad (6)$$

is diagonalized, are denoted MR $_{12}^{+T}$ -CISD(N), where $\vec{\alpha}$ is a cartesian vector of Dirac matrices, V_{iA} is the potential-energy operator for electron i in the electric field of nucleus A , $\mathbb{1}_4$ is a unit 4×4 matrix and V_{AB} represents the potential energy due to the internuclear classical electrostatic repulsion of the clamped nuclei, and N is the number of explicitly correlated electrons. For the model MR $_{12}^{+T}$ -CISD(10) the model parameter $n = 3$ is used in the present work. Details are to be found in reference [14].

For the determination of the nuclear magnetic hyperfine coupling the tantalum isotope ^{181}Ta is used for which the nuclear magnetic moment is $\mu = 2.361\mu_N$ [27]. Its nuclear spin quantum number is $I = 7/2$.

Results and discussion

Energetics and spectroscopic properties

Important characteristics of the active set of molecular four-spinors are displayed in Table I. The large similarities with the isoelectronic TaN system [14] are not surprising, but a number of important differences require special attention.

The energy difference $\left| \varepsilon_{\sigma_{6s}} - \varepsilon_{\delta_{5d_{3/2}}} \right| = 0.014 E_H$ (Kramers pairs 40 and 41) is significantly smaller than in TaN ($0.031 E_H$) and is a consequence of the increased nuclear charge on the neighboring light atom in TaO $^+$: An electron in a more diffuse Ta-localized $5d_{3/2}$ (or likewise $5d_{5/2}$) state experiences a greater stabilisation due the higher mean electrostatic potential than an electron in a more compact Ta-localized $6s_{1/2}$ state, leading to a differential energy shift of $-0.017 E_H \approx -3730 \text{ cm}^{-1}$. This relative stabilization of the Ta($5d$) spinors in TaO $^+$ is largely responsible for the change of electronic ground state compared to TaN, since the relative valence spinor occupation between the two states ($^1\Sigma_0^+$ and $^3\Delta_1$) predominantly corresponds to a transition $\sigma_{6s(1/2)}^1 \leftrightarrow \delta_{5d(3/2)}^1$.

TABLE I: Characterization of important active-space Kramers pairs in terms of orbital angular momentum projection, Dirac-Coulomb Hartree-Fock spinor energy, and principal atomic shell character based on a Mulliken population analysis at $3.1a_0$ internuclear distance; the Kramers pairs numbered 29-35 represent the Ta(4f) shell.

No.	$ m_j $	$\left \left\langle \hat{\ell}_z \right\rangle_{\varphi_i} \right $	$\varepsilon_{\varphi_i} [E_H]$	atomic population, Atom(ℓ_λ)
25	1/2	0.000	-3.507	99% Ta(s)
26	1/2	0.592	-2.337	38% Ta(p_σ), 59% Ta(p_π)
27	1/2	0.401	-2.028	51% Ta(p_σ), 40% Ta(p_π)
28	3/2	1.000	-1.981	100% Ta(p_π)
\vdots	\vdots	\vdots	\vdots	\vdots
36	1/2	0.006	-1.425	84% O(s), 7% Ta(p_σ), 5% Ta(d_σ)
37	1/2	0.021	-0.755	70% O(p_σ), 16% Ta(d_σ)
38	1/2	0.979	-0.737	74% O(p_π), 20% Ta(d_π)
39	3/2	1.000	-0.736	76% O(p_π), 20% Ta(d_π)
40	1/2	0.001	-0.570	79% Ta(s), 17% Ta(d_σ)
41	3/2	1.994	-0.556	100% Ta(d_δ)
42	5/2	2.000	-0.555	100% Ta(d_δ)
43	1/2	0.846	-0.175	53% Ta(p_π), 28% Ta(d_π), 8% Ta(p_σ)
44	3/2	1.003	-0.161	63% Ta(p_π), 33% Ta(d_π)
45	1/2	0.154	-0.151	44% Ta(p_π), 26% Ta(d_σ), 9% Ta(d_π), 7% Ta(d_σ)
46	1/2	0.991	-0.071	55% Ta(p_π), 33% Ta(d_π), 9% O(p_π)
47	3/2	1.003	-0.069	54% Ta(p_π), 35% Ta(d_π), 8% O(p_π)

Also in contrast to TaN (8% contribution) [14] and the corresponding spinor in the YbF molecule (13%) [28] a p -wave contribution to the valence $\sigma_{6s_{1/2}}$ spinor is quite small ($\approx 3\%$) in the TaO⁺ system. The fractionally occupied $\sigma_{6s_{1/2}}$ spinor is more strongly stabilized by an increase of nuclear charge on the neighboring atom than the virtual $\sigma_{6p_{1/2}}$ spinor (Kramers pair 43). As a consequence, the energy gap is increased and mixing of s - and p -waves reduced in TaO⁺. This fact has implications for the size of \mathcal{P} , \mathcal{T} -odd matrix elements in the $^3\Delta_1$ state and will be discussed in a following subsection.

Important information for experimentally preparing the system in the science state is given by the molecular constants, transition energies, and transition dipole moments for an ensemble of energetically low-lying electronic states. The seven lowest electronic states have been addressed in this work. An analysis of the corresponding CI wavefunctions and results for spectroscopic constants of these states are shown in Table II. Corresponding potential-energy curves are displayed in Fig. 1.

It is firmly established that $^3\Delta_1$ ($\sigma_{6s(1/2)_{\text{Ta}}}^1 \delta_{5d(3/2)_{\text{Ta}}}^1$) is the electronic ground state of the TaO⁺ molecular ion. The excitation energy of the $^1\Sigma_0^+$ state – the electronic ground state in the TaN system – of more than 3700 [cm⁻¹] is much too large to leave doubt about the principal state ordering. As a further confirmation of the above-discussed effect that leads to this state ordering, the spin-orbit splitting within the $^3\Delta$ multiplet is here about 20% larger than in TaN, which is again due to the increased nuclear charge on the neighboring light atom.

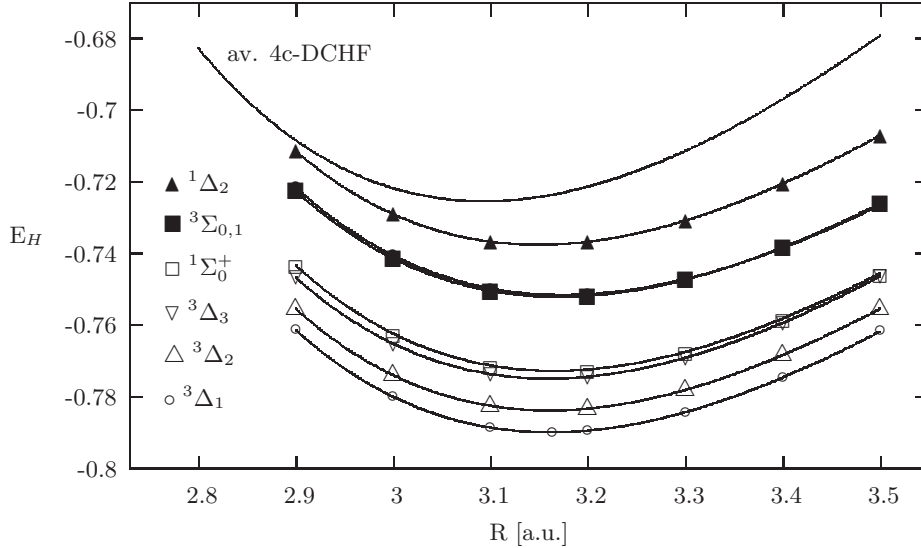
\mathcal{P} , \mathcal{T} -Odd Properties, Hyperfine Interaction and G-Tensor

Since TaO⁺ is an electronically paramagnetic system, the dominant sources of a potential \mathcal{P} , \mathcal{T} -odd effect are leptonic and semi-leptonic [2]. Among these, the pseudoscalar-scalar (PSS) and tensor-pseudotensor (TPT) contributions to the molecular EDM are estimated to be at least three orders of magnitude smaller than the ne-SPS contribution for many underlying models of (\mathcal{CP})-

TABLE II: Characterization of electronic ground and energetically lowest-lying excited states at an internuclear distance of $R = 3.1$ a₀; the wavefunction model used is MR₁₂^{+T}-CISD(10). The percentage is calculated as $100 \times \sum_j |C_j|^2$ for a normalized CI wavefunction, where j denotes a Slater determinant and the sum runs over determinants of the respective configuration. Spectroscopic constants; R_e the equilibrium internuclear distance, ω_e the harmonic vibrational frequency, B_e the rotational constant, and T_e the equilibrium excitation energy

$^{2S+1}\Lambda_\Omega$	$\lambda_{nl(\omega)_{\text{Atom}}^o}$, $\omega = m_j $, o : occupation	R_e [a.u.]	ω_e [cm ⁻¹]	B_e [cm ⁻¹]	T_e [cm ⁻¹]
$^3\Delta_1$	88% $\sigma_{6s(1/2)_{\text{Ta}}}^1 \delta_{5d(3/2)_{\text{Ta}}}^1$	3.161	1091	0.410	0
$^3\Delta_2$	59% $\sigma_{6s(1/2)_{\text{Ta}}}^1 \delta_{5d(3/2)_{\text{Ta}}}^1$, 29% $\sigma_{6s(1/2)_{\text{Ta}}}^1 \delta_{5d(5/2)_{\text{Ta}}}^1$	3.160	1092	0.410	1318
$^3\Delta_3$	88% $\sigma_{6s(1/2)_{\text{Ta}}}^1 \delta_{5d(5/2)_{\text{Ta}}}^1$	3.160	1093	0.410	3270
$^1\Sigma_0^+$	52% $\sigma_{6s(1/2)_{\text{Ta}}}^2$, 32% $\delta_{5d(3/2)_{\text{Ta}}}^2$, 2% $\delta_{5d(5/2)_{\text{Ta}}}^2$	3.165	1086	0.409	3759
$^3\Sigma_0^+$	12% $\sigma_{6s(1/2)_{\text{Ta}}}^2$, 40% $\delta_{5d(3/2)_{\text{Ta}}}^2$, 35% $\delta_{5d(5/2)_{\text{Ta}}}^2$	3.170	1071	0.408	8265
$^3\Sigma_1^+$	88% $\delta_{5d(3/2)_{\text{Ta}}}^1 \delta_{5d(5/2)_{\text{Ta}}}^1$	3.174	1061	0.407	8409
$^1\Delta_2$	27% $\sigma_{6s(1/2)_{\text{Ta}}}^1 \delta_{5d(3/2)_{\text{Ta}}}^1$, 57% $\sigma_{6s(1/2)_{\text{Ta}}}^1 \delta_{5d(5/2)_{\text{Ta}}}^1$	3.149	1101	0.413	11458

FIG. 1: Potential energy curves for the lowest-lying electronic state of TaO⁺, using the CI model MR₁₂^{+T}-CISD(10), cutoff 30 a.u. The energy offset is $-15671 E_H$.



violation [29], leaving the electron EDM and ne-SPS interaction as the main contributors.

At the calculated equilibrium internuclear distance and the best level of theory, the effective electric field for TaO⁺ is $E_{\text{eff}} = 20.2 \left[\frac{\text{GV}}{\text{cm}} \right]$ (see Table III) which is about 45% smaller than the value for TaN [14, 15]. The reason for this is the smaller p -wave contribution to the valence $\sigma_{6s_{1/2}}$ spinor in TaO⁺, leading to a smaller \mathcal{P} -odd matrix element. E_{eff} for TaO⁺ is about 27% of the value in the corresponding state for thorium monoxide [9, 10] which currently yields the strongest constraints on underlying BSM parameters [8]. The ne-SPS interaction constant in Table III is $W_S = 17.7$ [kHz], again about 45% smaller than the value for TaN which confirms internal consistency of the acquired results.

However, the two corresponding interaction constants W_d and W_S should be considered jointly when bounds on underlying (CP) -odd parameters are to be extracted [30]. Interestingly, the ratio $W_d/W_S = 276 \left[\frac{10^{18}}{e \text{ cm}} \right]$ found in the present work differs strongly from the respective ratios for the

TABLE III: Molecular electric dipole moment, EDM effective electric field, magnetic hyperfine interaction constant, scalar-pseudoscalar electron-nucleon interaction constant, nuclear magnetic quadrupole interaction constant and parallel g-tensor component at two internuclear distances R and with two different wavefunction models for the electronic ground state ${}^3\Delta_1$ ($\Omega = 1$)

CI Model, R	D [Debye]	E_{eff} [$\frac{\text{GV}}{\text{cm}}$]	$A_{ }$ [MHz]	W_S [kHz]	W_M [$\frac{10^{33}\text{Hz}}{e\text{cm}^2}$]	$G_{ }$ [a.u.]
MR $_{12}^{+T}$ -CISD(10), 3.1 a_0	-3.91	17.6	-4537	15.7	0.38	0.0024
MR $_{12}^{+T}$ -CISD(18), 3.1 a_0	-3.85	20.7	-4593	18.4	0.46	0.0025
MR $_{12}^{+T}$ -CISD(10), 3.1609 a_0	-4.08	17.0	-4492	15.1	0.37	0.0030
MR $_{12}^{+T}$ -CISD(18), 3.1609 a_0	-4.01	20.2	-4544	17.7	0.45	0.0032

ThO system [9], $W_d/W_S = 172 \left[\frac{10^{18}}{e\text{cm}} \right]$ and the ThF $^+$ system [20], $W_d/W_S = 176 \left[\frac{10^{18}}{e\text{cm}} \right]$. With the present dominant sources the \mathcal{P}, \mathcal{T} -odd energy shift is written as

$$\Delta\varepsilon_{\mathcal{P},\mathcal{T}} = \frac{1}{2} (W_d d_e + W_c C_S) \langle \mathbf{n} \cdot \mathbf{e}_z \rangle (E_{\text{ext}}) \quad (7)$$

where \mathbf{n} is the unit vector along the molecular axis and the external electric field is assumed to be along the z axis in the laboratory frame. The parameter W_c is related to W_S as $W_c = \frac{A}{2Z} W_S$, where A is the nucleon and Z is the proton number [31]. This means that an accurate measurement of an upper bound to $\Delta\varepsilon_{\mathcal{P},\mathcal{T}}(\text{TaO}^+)$ in combination with the present values for the interaction constants W_d and W_S and the corresponding data for the ThO system would lead to stronger constraints on the BSM parameters d_e and C_S .

The nuclear MQM interaction constant $W_M = 0.45 \left[\frac{10^{33}\text{Hz}}{e\text{cm}^2} \right]$ for TaO $^+$ given in Table III is about 40% smaller than the one for the isoelectronic TaN system [14], but still sizeable. In combination with an accurate measurement of a \mathcal{P}, \mathcal{T} -odd energy shift in the molecular ion it could be used to constrain nuclear (\mathcal{CP})-odd BSM parameters. Following the calculations in Ref. [16] the expected energy shift in ${}^{181}\text{TaO}^+$ due to $|W_M M|$, where M is the nuclear magnetic quadrupole moment, is $< 150 \mu\text{Hz}$ with respect to the proton EDM, $|d_p|$, as an underlying source. Correspondingly, taking the limits on the QCD (\mathcal{CP})-violating parameter $|\tilde{\Theta}|$ and the difference of the quark chromo-EDMs, $|\tilde{d}_u - \tilde{d}_d|$, the shifts $|W_M M|$ correspond to $< 70 \mu\text{Hz}$ and $< 100 \mu\text{Hz}$, respectively. Given that the current uncertainty on the \mathcal{P}, \mathcal{T} -odd energy shift of $800 \mu\text{Hz}$ in ThO could ultimately be improved by two orders of magnitude [8, 32], an experiment of similar accuracy on TaO $^+$ would probe (\mathcal{CP})-violating physics in the hadron sector.

The parallel component of the G-tensor in the ${}^3\Delta_1$ state of TaO $^+$, $G_{||} = 0.0032$ a.u., is very small, even for a ${}^3\Delta$ molecule in the $\Omega = 1$ state, and has about the same size as $G_{||}$ in ThO (${}^3\Delta_1$) [33]; the experimental value is $g_H = 0.0044$ a.u. [34]. For comparison, $G_{||} \approx 0.03$ a.u. for ThF $^+$ (${}^3\Delta_1$) is an order of magnitude larger [33, 35]. The present finding is reasonable because there is no electronic state available in TaO $^+$ within an energy window of more than 10000 cm^{-1} allowed to mix with ${}^3\Delta_1$ *via* second-order spin-orbit interaction selection rules, see Tables II and IV. Due to this small mixing $G_{||}$ is close to $g_s - 2$. This situation is qualitatively different in the ThF $^+$ system [20].

A consistent trend is observed for the parallel magnetic hyperfine constants when comparing TaO $^+$ with three other molecular EDM candidates. On the absolute, $A_{||}$ for ${}^{229}\text{Th}$ increases by about 45% from ThO [11] to the isoelectronic ion with the heavier partner nucleus, ThF $^+$ [20]. Likewise, the replacement of the nitrogen by an oxygen nucleus on the neighboring atom increases $A_{||}$ for ${}^{229}\text{Ta}$ by about 54%. A corresponding measurement would reveal how well the spin density close to the heavy nucleus is described by the present molecular wavefunctions which in turn would yield information on the accuracy of the presented \mathcal{P}, \mathcal{T} -odd interaction constants.

Finally, the center-of-mass molecular static electric dipole moment in TaO $^+$ (${}^3\Delta_1$) of $-4.01 [D]$ is large and allows for near complete polarization of the system in weak external electric fields, for instance by the use of ion traps and rotating electric fields [36].

TABLE IV: Molecule-frame static electric dipole moments $\langle {}^M\Lambda_\Omega | \hat{D}_z | {}^M\Lambda_\Omega \rangle$, transition dipole moments $\left| \left\langle {}^M\Lambda'_\Omega | \hat{D} | {}^M\Lambda_\Omega \right\rangle \right|$, with \hat{D} the electric dipole moment operator (both in Debye units), using the model MR $_{12}^{+T}$ -CISD(10). The origin is at the center of mass, and the internuclear distance is $R = 3.1609 [a_0]$ (O nucleus placed at $z\vec{e}_z$ with $z > 0$). Transition dipole moments smaller than 10^{-7} Debye are not shown.

${}^M\Lambda_\Omega$ State	${}^3\Delta_1$	${}^3\Delta_2$	${}^3\Delta_3$	${}^1\Sigma_0^+$	${}^3\Sigma_0^+$	${}^3\Sigma_1^+$	${}^1\Delta_2$
${}^3\Delta_1$	-4.077						
${}^3\Delta_2$	0.041	-4.044					
${}^3\Delta_3$	-	0.041	-4.043				
${}^1\Sigma_0^+$	0.036	-	-	-4.109			
${}^3\Sigma_0^+$	0.108	-	-	0.716	-4.960		
${}^3\Sigma_1^+$	0.006	0.087	-	0.040	0.000	-5.341	
${}^1\Delta_2$	0.131	0.131	0.098	-	-	0.071	-3.309

CONCLUSION

In the present work a new molecular ionic system is proposed as a candidate for the detection of an EDM signal. TaO $^+$ provides all the advantages of molecules in ${}^3\Delta_1$ states exploited in leading EDM experiments [8, 36] and may be used for probing (\mathcal{CP})-violation beyond the standard model in both the lepton and the hadron sectors. The obtained \mathcal{P} , \mathcal{T} -odd molecular enhancements are smaller than the ones in the ThO and the isoelectronic TaN systems, but this disadvantage may be overcompensated by the fact that the ${}^3\Delta_1$ state is the electronic ground state of TaO $^+$, allowing for an in principle infinite measurement time. The only other paramagnetic molecule currently considered for EDM experiments which has a ${}^3\Delta_1$ ground state is ThF $^+$ [20, 37]. However, TaO $^+$ only has a factor of 2-3 smaller \mathcal{P} , \mathcal{T} -odd constants but an order of magnitude smaller magnetic moment in ${}^3\Delta_1$ than the latter.

In reference [16] the TaN system has been graded as “especially promising”. Given the present findings, the isoelectronic TaO $^+$ system is even more so.

The *Agence Nationale de la Recherche* (ANR) through grant no. ANR-BS04-13-0010-01, project “EDMeDM”, is thanked for financial support. Moreover, I wish to thank David DeMille (Yale) for an inspiring discussion.

-
- * Electronic address: timo.fleig@irsamc.ups-tlse.fr
- [1] J. Engel, M. J. Ramsey-Musolf, and U. van Kolck. Electric dipole moments of nucleons, nuclei, and atoms: The Standard Model and beyond. *Prog. Part. Nuc. Phys.*, 71:21, 2013.
 - [2] I. B. Khriplovich and S. K. Lamoreaux. *CP Violation Without Strangeness*. Springer; Berlin, Heidelberg, 1997.
 - [3] M. Pospelov and A. Ritz. Electric dipole moments as probes of new physics. *Ann. Phys.*, 318:119, 2005.
 - [4] J. S. M. Ginges and V. V. Flambaum. Violations of fundamental symmetries in atoms and tests of unification theories of elementary particles. *Phys. Rev.*, 397:63, 2004.
 - [5] M. Kobayashi and T. Maskawa. CP violation in the renormalizable theory of weak interaction. *Prog. Theor. Phys.*, 49:652, 1973.
 - [6] T. Chupp and M. Ramsey-Musolf. Electric dipole moments: A global analysis. *Phys. Rev. C*, 91:035502, 2015.
 - [7] M. Jung. A robust limit for the electric dipole moment of the electron. *J. High Energy Phys.*, 5:168, 2013.
 - [8] The ACME Collaboration, J. Baron, W. C. Campbell, D. DeMille, J. M. Doyle, G. Gabrielse, Y. V. Gurevich, P. W. Hess, N. R. Hutzler, E. Kirilov, I. Kozyryev, B. R. O’Leary, C. D. Panda, M. F. Parsons, E. S. Petrik, B. Spaun, A. C. Vutha, and A. D. West. Order of Magnitude Smaller Limit on the Electric Dipole Moment of the Electron. *Science*, 343:269, 2014.
 - [9] M. Denis and T. Fleig. In search of discrete symmetry violations beyond the standard model: Thorium monoxide reloaded”. *J. Chem. Phys.*, 145:028645, 2016.
 - [10] L. V. Skripnikov and A. V. Titov. Theoretical study of ThO for the electron electric dipole moment search: Electronic properties of $H^3\Delta_1$ in ThO. *J. Chem. Phys.*, 142:024301, 2015.
 - [11] T. Fleig and M. K. Nayak. Electron electric dipole moment and hyperfine interaction constants for ThO. *J. Mol. Spectrosc.*, 300:16, 2014.
 - [12] R. J. Crewther, P. di Vecchia, G. Veneziano, and E. Witten. Chiral estimate of the electric dipole moment of the neutron in quantum chromodynamics. *Phys. Lett. B*, 88:123, 1979.
 - [13] J. F. Gunion and D. Wyler. Inducing a large neutron electric dipole moment via a quark chromoelectric dipole moment. *Phys. Lett. B*, 248:170, 1990.
 - [14] T. Fleig, M. K. Nayak, and M. G. Kozlov. TaN, a molecular system for probing P,T-violating hadron physics. *Physical Review A*, 93:012505, January 2016.
 - [15] L. V. Skripnikov, A. N. Petrov, N. S. Mosyagin, A. V. Titov, and V. V. Flambaum. TaN molecule as a candidate for the search for a T,P -violating nuclear magnetic quadrupole moment. *Phys. Rev. A*, 92:012521, 2015.
 - [16] V. V. Flambaum, D. DeMille, and M. G. Kozlov. Time-Reversal Symmetry Violation in Molecules Induced by Nuclear Magnetic Quadrupole Moments. *Phys. Rev. Lett.*, 113:103003, 2014.
 - [17] L. V. Skripnikov, A. N. Petrov, A. V. Titov, and V. V. Flambaum. CP -Violating Effect of the Th Nuclear Magnetic Quadrupole Moment: Accurate Many-Body Study of ThO. *Phys. Rev. Lett.*, 113:263006, 2014.
 - [18] E. Lindroth, B. W. Lynn, and P. G. H. Sandars. Order α^2 theory of the atomic electric dipole moment due to an electric dipole moment on the electron. *J. Phys. B*, 22:559, 1989.
 - [19] T. Fleig and M. K. Nayak. Electron electric-dipole-moment interaction constant for HfF^+ from relativistic correlated all-electron theory. *Phys. Rev. A*, 88:032514, 2013.
 - [20] M. Denis, M. Nørby, H. J. Aa. Jensen, A. S. P. Gomes, M. K. Nayak, S. Knecht, and T. Fleig. Theoretical study on ThF^+ , a prospective system in search of time-reversal violation. *New J. Phys.*, 17:043005, 2015.
 - [21] P. J. Mohr, D. B. Newell, and B. N. Taylor. CODATA recommended values of the fundamental physical constants: 2014. arXiv:1507.07956v1 [physics.atom-ph], 2014.
 - [22] DIRAC, a relativistic ab initio electronic structure program, Release DIRAC15 (2015), written by R. Bast, T. Sauer, L. Visscher, and H. J. Aa. Jensen, with contributions from V. Bakken, K. G. Dyall, S. Dubillard, U. Ekstroem, E. Eliav, T. Enevoldsen, E. Fasshauer, T. Fleig, O. Fossgaard, A. S. P. Gomes, T. Helgaker, J. Henriksson, M. Ilias, Ch. R. Jacob, S. Knecht, S. Komorovsky, O. Kullie, J. K. Laerdahl, C. V. Larsen, Y. S. Lee, H. S. Nataraj, M. K. Nayak, P. Norman, G. Olejniczak, J. Olsen, Y. C. Park, J. K. Pedersen, M. Pernpointner, R. Di Remigio, K. Ruud, P. Salek, B. Schimmelpennig, J. Sikkema, A. J. Thorvaldsen, J. Thyssen, J. van Stralen, S. Villaume, O. Visser, T. Winther, and S. Yamamoto (see <http://www.diracprogram.org>).
 - [23] S. Knecht, H. J. Aa. Jensen, and T. Fleig. Large-Scale Parallel Configuration Interaction. II. Two- and four-component double-group general active space implementation with application to BiH. *J. Chem. Phys.*, 132:014108, 2010.
 - [24] K. G. Dyall. Relativistic double-zeta, triple-zeta, and quadruple-zeta basis sets for the 5d elements Hf-Hg. *Theoret. Chim. Acta*, 112:403, 2004.
 - [25] K. G. Dyall and A. S. P. Gomes. Revised relativistic basis sets for the 5d elements Hf-Hg. *Theoret.*

- Chim. Acta*, 125:97, 2010.
- [26] T. H. Jr. Dunning. Gaussian basis sets for use in correlated molecular calculations. I. the atoms boron through neon and hydrogen. *J. Chem. Phys.*, 90:1007, 1989.
 - [27] L. C. Erich, A. C. Gossard, and R. L. Hartless. Magnetic moment of ^{181}Ta . *J. Chem. Phys.*, 59:3911, 1973.
 - [28] Timo Fleig, unpublished.
 - [29] S. M. Barr. T - and P -odd electron-nucleon interactions and the electric dipole moments of large atoms. *Phys. Rev. D*, 45:4148, 1992.
 - [30] M. Jung and A. Pich. Electric Dipole Moments in Two-Higgs-Doublet Models. *J. High Energy Phys.*, 4:076, 2014.
 - [31] V. A. Dzuba, V. V. Flambaum, and C. Harabati. Relations between matrix elements of different weak interactions and interpretation of the parity-nonconserving and electron electric-dipole-moment measurements in atoms and molecules. *Phys. Rev. A*, 84:052108, Nov 2011.
 - [32] David DeMille (Yale). private communication.
 - [33] M. Denis and T. Fleig. A Survey of Properties in EDM Candidate Molecules. to be submitted., 2017.
 - [34] E. Kirilov, W. C. Campbell, J. M. Doyle, G. Gabrielse, Y. V. Gurevich, P. W. Hess, N. R. Hutzler, B. R. O'Leary, E. Petrik, B. Spaun, A. C. Vutha, and D. DeMille. Shot-noise-limited spin measurements in a pulsed molecular beam. *Phys. Rev. A*, 88:013844, 2013.
 - [35] K. Balasubramanian. The low-lying states of the second-row transition metal hydrides (YH-CdH). *J. Chem. Phys.*, 93:8061, 1990.
 - [36] H. Loh, K. Cossel, M. C. Grau, K.-K. Ni, E. R. Meyer, J. L. Bohn, J. Ye, and E. A. Cornell. Precision Spectroscopy of Polarized Molecules in an Ion Trap. *Science*, 342:1220, 2013.
 - [37] D. N. Gresh, K. C. Cossel, Y. Zhou, J. Ye, and E. A. Cornell. Broadband velocity modulation spectroscopy of ThF^+ for use in a measurement of the electron electric dipole moment. *J. Mol. Spectrosc.*, 319:1, 2016.